> Ir > Co > Ru, Os.[9] These observations, together with the M–N bond distances and other facts mentioned above, indicate that the most active catalysts are those metals which have the greatest tendency to back-donate electrons to the ligands. This electron transfer would tend to make the presumed five-coordinate catalytic intermediates[9,10] more reactive and could provide the driving force for the coupling of the nitrosyl groups, thus increasing catalytic activity. Back-donation into NO π^* orbitals should also make the oxygen transfer in reaction 1 more facile.

We believe that the structural differences observed in this series of complexes primarily result from the different electronic requirements of the metals, as the packing forces around the metal atoms should be very similar. The structural trends are consistent with the observed catalytic behavior and may provide some help in elucidating a mechanism for the catalysis of reaction 1 by systems containing these complexes.

Acknowledgment. We wish to thank Matthey-Bishop, Inc., for the generous loan of precious metals used in our studies. We also wish to thank Dr. B. L. Haymore for his helpful advice and comments. J.A.K. wishes to acknowledge the support of an NSF predoctoral fellowship. This work was supported by the National Science Foundation.

Registry No. $[Rh(NO)_2(P(C_6H_5)_3)_2][ClO_4]$, 47841-81-6; $Rh(NO)(PPh_3)_3$, 21558-94-1.

Supplementary Material Available. Table III, the structure amplitudes, will appear following these pages in the microfilm edition of this volume of the journal. Photocopies of the supplementary material from this paper only or microfiche (105 × 148 mm, 24× reduction, negatives) containing all of the supplementary material for papers in this issue may be obtained from the Business Office, Books and Journals Division, American Chemical Society, 1155 16th St., N.W., Washington, D.C. 20036. Remit check or money order for $4.50 for photocopy or $2.50 for microfiche, referring to code number AIC504584-12-75.

References and Notes

(1) V. G. Albano, A. Araneo, P. L. Bellon, G. Ciani, and M. Manassero, *J. Organomet. Chem.*, **67**, 413 (1974).
(2) A. P. Gaughan, B. J. Corden, R. Eisenberg, and J. A. Ibers, *Inorg. Chem.*, **13**, 786 (1974).
(3) S. Bhaduri and G. M. Sheldrick, *Acta Crystallogr., Sect. B*, **31**, 897 (1975).
(4) B. L. Haymore and J. A. Ibers, *Inorg. Chem.*, **14**, 2610 (1975).
(5) J. C. Huffman, private communication.
(6) D. M. P. Mingos and J. A. Ibers, *Inorg. Chem.*, **9**, 1105 (1970).
(7) B. F. G. Johnson and S. Bhaduri, *J. Chem. Soc., Chem. Commun.*, 650 (1973).
(8) B. L. Haymore and J. A. Ibers, *J. Am. Chem. Soc.*, **96**, 3325 (1974).
(9) J. A. Kaduk, B. L. Haymore, and J. A. Ibers, unpublished observations.
(10) B. F. G. Johnson, C. J. Savory, J. A. Segal, and R. H. Walter, *J. Chem. Soc., Chem. Commun.*, 809 (1974).
(11) For other studies on the catalysis of reaction 1, see R. Eisenberg and C. D. Meyer, *Acc. Chem. Res.*, **8**, 26 (1975), and references therein.
(12) J. J. Levinson and S. D. Robinson, *J. Chem. Soc. A*, 2947 (1970).
(13) R. J. Doedens and J. A. Ibers, *Inorg. Chem.*, **6**, 204 (1967).
(14) In addition to various local programs for the CDC 6400, computer programs used in this work include local versions of Zalkin's FORDAP Fourier program, the AGNOST absorption program, and Busing and Levy's ORFFE function and error program. Our least-squares program NUCLS, in its nongroup form, closely resembles the Busing–Levy ORFLS program.
(15) D. T. Cromer and J. T. Waber, "International Tables for X-Ray Crystallography", Vol. IV, Kynoch Press, Birmingham, England, 1974, Table 2.2A; D. T. Cromer and D. Liberman, *J. Chem. Phys.*, **53**, 1891 (1970).
(16) See, for example, R. Eisenberg and J. A. Ibers, *Inorg. Chem.*, **4**, 773 (1965).
(17) Supplementary material.

Contribution from the Department of Chemistry,
Northwestern University, Evanston, Illinois 60201

A Fumaronitrile Complex of Rhodium(I). Structure of Iodo(fumaronitrile)(triphenyl phosphite)bis(*p*-methoxyphenyl isocyanide)rhodium(I), $RhI(\textit{trans}\text{-}H(NC)C{=}C(CN)H)(P(OC_6H_5)_3)(p\text{-}CH_3OC_6H_4NC)_2$

ARTHUR P. GAUGHAN, Jr., and JAMES A. IBERS*

Received July 18, 1975 AIC505139

The solid-state structure of the title complex which exhibits dynamic solution behavior has been determined from three-dimensional X-ray data collected by counter techniques. The material crystallizes in space group C_{2h}^5-$P2_1/c$ of the monoclinic system with four molecules of the complex in the unit cell. Crystal data are a = 15.252 (7) Å, b = 11.454 (6) Å, c = 21.933 (11) Å, β = 103.62 (2)°, and V = 3723.7 Å^3. The observed and calculated (Z = 4) densities are 1.57 (2) and 1.577 g/cm^3, respectively. The structure, including the H atoms of the fumaronitrile ligand, has been refined (on F) by a full-matrix least-squares procedure to a conventional agreement index of 0.040 for 4357 observations having $F_o^2 > 3\sigma(F_o^2)$. The structural results reveal trigonal-bipyramidal coordination about the Rh atom with trans-axial isocyanide ligands (C–Rh–C = 177.7 (2)°) situated at 1.964 Å (average) from the metal. The equatorial plane contains an iodo, a triphenyl phosphite, and a symmetrically π-bonded fumaronitrile ligand. The olefinic carbon atoms lie almost exactly in the plane defined by Rh, I, and P (average deviation 0.05 Å) and are equidistant from the metal: Rh–C = 2.139 Å (average). The distance from the Rh atom to the midpoint of the olefinic bond (Ct) is 2.013 Å. There is considerable angular distortion in the equatorial plane: I–Rh–P = 102.37 (5)°, I–Rh–Ct = 118.9 (2)°, and P–Rh–Ct = 138.7 (2)°. The distortions within the olefin are about as expected: the olefinic C–C distance is 1.444 (10) Å and the substituents are bent back and away from the metal center by 28° (average). Other distances of interest are Rh–P = 2.265 (2) Å and Rh–I = 2.739 (2) Å. The implications of the solid-state structure on the interpretation of the dynamic solution behavior of this and related complexes are discussed.

Introduction

Solid-state structures of isolable transition metal–olefin complexes are useful models for the interaction of the olefinic bond with transition metals in homogenously catalytic reactions. Spectroscopic studies of the various dynamical processes that certain of such complexes undergo in solution provide valuable insight into the possibly facile and important rearrangements that occur during such reactions. Generally these isolable complexes contain olefins substituted with various electron-withdrawing groups, such as halogen or cyanide. As a result the determination by X-ray diffraction of the metrical details of the metal–olefin interaction is facilitated. In addition the activated olefinic systems are of intrinsic interest because they occasionally mimic the catalytically induced hydrogenation of simple olefins.[1]

Over the past decade a large number of accurate transition metal–olefin structures have been reported. In particular, those of d^8 metals in complexes containing monodentate ligands have

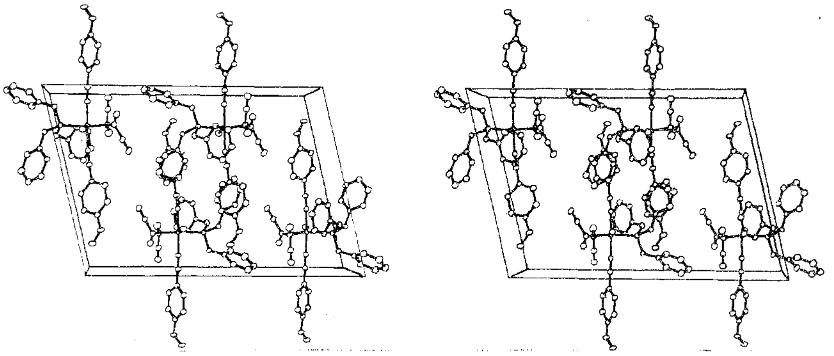

Figure 1. A stereoscopic view of the contents of the unit cell of RhI(*trans*-$H(NC)C{=}C(CN)H)(P(OC_6H_5)_3)(p\text{-}CH_3OC_6H_4NC)_2$. The origin is at the lower left rear. The *x* axis is vertical, the *z* axis is horizontal, and the *y* axis points out of the plane of the paper. The shapes of the atoms represent 20% contours of thermal motion. All H atoms except those of the fumaronitrile ligand have been omitted for the sake of clarity.

been shown to be trigonal bipyramidal with the olefinic carbon atoms in the equatorial plane and essentially equidistant from the metal. Recently, Kaneshima et al.[2] have prepared a series of new d^8 transition metal–cyanoolefin complexes containing isocyanide ligands and they have studied the dynamics of rearrangement of certain of these complexes in solution. Their results indicate that the dynamic behavior of these complexes is markedly dependent upon the nature of the other ligands bonded to the metal center. They have interpreted their results in some instances to indicate that the cyanoolefin is undergoing hindered rotation about the coordination bond either in a tetragonal pyramid or in a trigonal bipyramid. If the coordination geometry is that of a trigonal bipyramid, then the olefin rotation accompanies a Berry pseudorotation of the other four ligands. In view of the propensity of five-coordinate d^8 metal complexes to assume a trigonal-bipyramidal geometry and those of d^6 metals to be tetragonal pyramids the possibility of a d^8 tetragonal pyramid would indicate a unique metal–olefin interaction. Consequently, a structural study of one such complex seems warranted. The results are presented here.

Experimental Section

Crystals of RhI(*trans*-$H(NC)C{=}C(CN)H)(P(OC_6H_5)_3)(p\text{-}CH_3OC_6H_4NC)_2$, which exhibits dynamic behavior in solution,[3] were kindly supplied by K. Kawakami and were suitable without recrystallization. Preliminary characterization of the material was undertaken employing precession and Weissenberg techniques. A total of 7265 intensity data including space group extinct and equivalent reflections were collected by the θ–2θ scan technique on a computer-controlled Picker FACS-1 automatic diffractometer. Crystallographic and data collection details are given in Table I. The data processing was carried out as previously described.[4,5] The value of *p* was 0.04. The appropriate members of $\{hkl\}$ in the inner core of complete data ($3° \le 2\theta \le 15°$) were averaged under the point group $C_{2h}{}^6$. The *R* index for averaging was 1.1%. The data were then corrected for absorption.[7] The transmission coefficients varied from 0.760 to 0.841. The inner data were again averaged yielding an *R* index of 0.9%. Only the 4357 unique data with $F_o^2 > 3\sigma(F_o^2)$ were used in the ensuing solution and refinement.

The structure was solved by direct methods using a symbolic addition procedure.[7] Two hundred and forty-nine normalized structure factors with $E \ge 1.76$ were utilized in the initial sign-determining process. The subsequent *E* map yielded trial positions for the heavy atoms as well as a variety of light-atom fragments. The complete trial structure was obtained from a subsequent structure factor–difference Fourier calculation. The ensuing refinement was uneventful. The final model involves anisotropic thermal parameters for the 20 nongroup, nonhydrogen atoms, individual isotropic thermal parameters for the five rigid phenyl groups,[8] and isotropic thermal parameters for the hydrogen atoms of the fumaronitrile ligand. The hydrogen atoms of the phenyl rings and the methyl groups were located on difference Fourier maps, idealized,[9] and added as fixed contributions in the final least-squares refinement. This refinement (on *F*) of 249 variables over 4357 data converged to *R* and R_w indices of 0.040 and 0.048, respectively. The maximum electron density on a subsequent difference Fourier map was 0.82 (9) e/Å^3, about 15% of the height of a typical carbon atom in this structure. An analysis of $\sum w(|F_o| - |F_c|)^2$ for various classes of reflections based on Miller indices, $|F_o|$, and setting angles shows no significant dependence on any of these quantities. The final error in an observation of unit weight is 1.38 e. A tabulation of $10|F_o|$ and $10|F_c|$ for those reflections used in the refinement has been deposited.[10,11] Of the 2214 reflections having $F_o^2 < 3\sigma(F_o^2)$ which were omitted from the refinement, nine had $|F_o^2 - F_c^2| > 3\sigma(F_o^2)$ and none had $|F_o^2 - F_c^2| > 4\sigma(F_o^2)$.

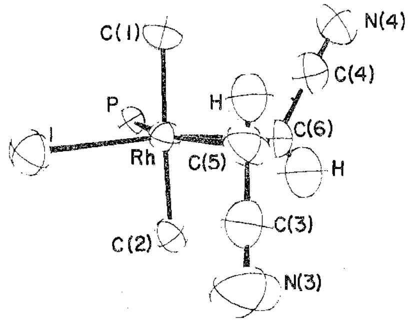

Figure 2. A perspective view of the inner coordination sphere of RhI(*trans*-$H(NC)C{=}C(CN)H)(P(OC_6H_5)_3)(p\text{-}CH_3OC_6H_4NC)_2$. The 50% probability ellipsoids are shown.

Table II lists the final positional and thermal parameters for the nongroup atoms and Table III gives the rigid-group parameters as well as the derived positions for the group atoms. A tabulation of the idealized positions for the hydrogen atoms is available.[11] In Table IV the root-mean-square amplitudes of those atoms refined anisotropically are presented.

Description of the Structure and Comparison with Related Complexes

The crystal structure consists of the packing of individual molecules of RhI(*trans*-$H(NC)C{=}C(CN)H)(P(OC_6H_5)_3)(p\text{-}CH_3OC_6H_4NC)_2$ situated at the general equipoints of the space group. All intermolecular contacts are normal. The molecular packing is dominated by van der Waals type interactions between phenyl substituents on both the triphenyl phosphite and *p*-methoxyphenyl isocyanide ligands of adjacent molecules. The resulting arrangement is depicted in a stereoview of the unit cell in Figure 1.

Selected intramolecular distances and angles will be found in Table V and a perspective view of the inner coordination sphere is shown in Figure 2. As might have been anticipated the arrangement of coordinated ligands about the Rh atom is trigonal bipyramidal[12] with axial *p*-methoxyphenyl isocyanide groupings and an equatorial plane consisting of an iodo, a triphenyl phosphite, and a fumaronitrile ligand. The principal angular distortions that occur in the trigonal-bipyramidal description are localized in the equatorial plane (Figure 3) for which a convenient rationale exists (vide infra).

The ligand set in the present complex is somewhat unusual:

Table I. Crystallographic and Data Collection Details for RhI(*trans*-H(NC)C=C(CN)H)(P(OC$_6$H$_5$)$_3$)(*p*-CH$_3$OC$_6$H$_4$NC)$_2$

	Crystal Data
Molecular formula	C$_{38}$H$_{31}$IN$_4$O$_5$PRh; mol wt 884.48
Unit cell (22°)	$a = 15.252$ (7) Å, $b = 11.454$ (6) Å, $c = 21.933$ (11) Å, $\beta = 103.62$ (2)°, $V = 3723.7$ Å^3, λ(Mo Kα_1) 0.70930 Å
Density	$d_{\text{measd}} = 1.57$ (2) g/cm^3, $d_{\text{calcd}} = 1.577$ g/cm^3; $Z = 4$; μ(Mo Kα) = 13.58 cm^{-1}
Space group	C_{2h}^5-$P2_1/c$
Morphology	{001}, {100}, {$\bar{1}$02}, {110}, (012), (0$\bar{1}$2); $V = 7.84 \times 10^{-3}$ mm^3
	Data Collection
Radiation	Mo K$\bar{\alpha}$
Monochromator	Graphite, (002)
Takeoff angle	1.9°
Crystal mounting	~7° off [010]
Scan rate	2°/min
Receiving aperture	4.7 mm wide × 4.3 mm high, 32 cm from crystal
Data collection limits	3° ≤ 2θ ≤ 15°, {*hkl*}; 15° < 2θ < 49°, ±*h*,+*k*,+*l*
Scan range (−Kα_1, +Kα_2)	0.75°, 0.75°
Background times	10 sec at scan limits 3° ≤ 2θ ≤ 38°; 20 sec at scan limits 38° < 2θ ≤ 49°
Attenuators	Cu foil, ratio ≅2.3; inserted at 7000 counts/sec
Standards	6 every 100 reflections; all within 3σ
No. of data	4357 space group unique reflections with $I > 3\sigma(I)$

there have been few structural determinations of transition metal complexes involving fumaronitrile, triphenyl phosphite, or iodo ligands, and none to our knowledge involving *p*-methoxyphenyl isocyanide. The Rh–I distance, 2.739 (2) Å, is in good agreement with other M–I (M = metal) distances found in comparable d^8 and formally d^6 complexes: 2.707 (1) Å in Pt(CH$_3$)(P(C$_6$H$_5$)$_3$)$_2$I·SO$_2$,[13] 2.666 (3) Å in [IrI(NO)(CO)(P(C$_6$H$_5$)$_3$)$_2$]$^+$,[14] 2.726 (2) Å in IrI(CH$_3$)(NO)(P(C$_6$H$_5$)$_3$)$_2$,[15] and 2.767 (5) Å in IrI(O$_2$)(CO)(P(C$_6$H$_5$)$_3$)$_2$.[16] The Rh–P distance, 2.265 (2) Å, is somewhat shorter than the M–P distances found in a number of four- and five-coordinate P(C$_6$H$_5$)$_3$ complexes of Rh[17–19] and Ir.[20] The M–P distances in these systems range from 2.315 (8) to 2.408 (3) Å. Although a direct comparison between the Rh–P distances in the present complex and its P(C$_6$H$_5$)$_3$ analogue[2] is not possible as was the case in Cr(CO)$_5$L[21] (L = P(C$_6$H$_5$)$_3$, P(OC$_6$H$_5$)$_3$), the short Rh–P distance is consistent with the notion[21] that P(OC$_6$H$_5$)$_3$ by virtue of the highly electronegative O atoms is capable of a stronger π-bonding interaction with a metal center than is P(C$_6$H$_5$)$_3$.

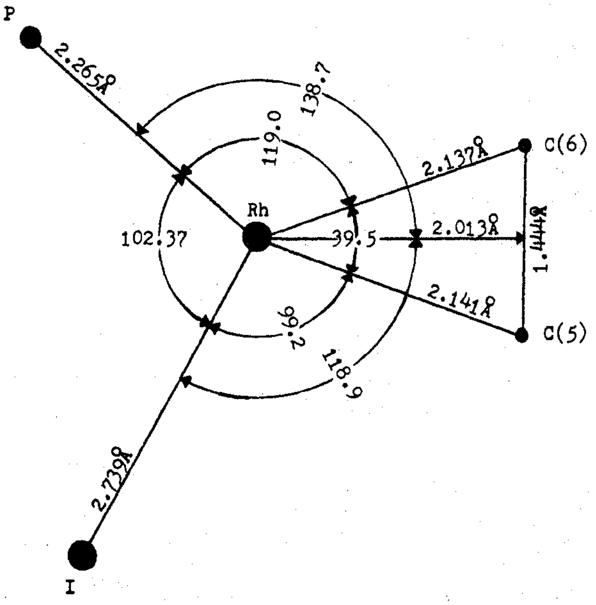

Figure 3. Metrical details of the equatorial plane in RhI(*trans*-H(NC)C=C(CN)H)P(OC$_6$H$_5$)$_3$(*p*-CH$_3$OC$_6$H$_4$NC)$_2$.

The averaged P–O and O–C(phenyl) distances, 1.599 (5) and 1.377 (7) Å, respectively, agree within experimental error with averaged values for Cr(CO)$_5$P(OC$_6$H$_5$)$_3$[21] and *trans*-Cr(CO)$_4$(P(OC$_6$H$_5$)$_3$)$_2$.[22] The Rh–P–O and O–P–O angles of the P(OC$_6$H$_5$)$_3$ ligand on the average show an ca. 9° expansion and contraction, respectively, relative to the tetrahedral value. Similar distortions are found in Cr(CO)$_5$P(OC$_6$H$_5$)$_3$,[21] Cr(CO)$_4$(P(OC$_6$H$_5$)$_3$)$_2$,[22] and *cis*-Fe$_2$(C$_5$H$_5$)$_2$(CO)$_3$P(OC$_6$H$_5$)$_3$,[23] suggesting that this is a general feature of P(OC$_6$H$_5$)$_3$ complexes. These distortions are reminiscent of a similar effect in the M–P–C and C–P–C angles of P(C$_6$H$_5$)$_3$ complexes[24,25] where the magnitude of the distortion is less, ca. 5°. Since P(OC$_6$H$_5$)$_3$ is less sterically hindered than P(C$_6$H$_5$)$_3$, it appears that this effect is electronic

Table II. Positional and Thermal Parameters for the Nongroup Atoms of RhI(*trans*-H(NC)C=C(CN)H)P(OC$_6$H$_5$)$_3$(*p*-CH$_3$OC$_6$H$_4$NC)$_2$

ATOM	X[A]	Y	Z	B11[B] OR B,A^2	B22	B33	B12	B13	B23
RH	0.211612(28)	0.314634(41)	0.374876(21)	30.01(21)	67.35(42)	16.43(11)	-0.16(24)	3.69(11)	0.20(18)
I	0.234410(30)	0.550691(36)	0.391216(22)	56.07(26)	64.41(39)	31.38(14)	1.76(24)	2.88(15)	3.19(18)
P	0.207290(98)	0.25320(13)	0.472304(70)	36.24(73)	64.0(13)	17.36(37)	-1.03(78)	4.93(42)	-1.86(56)
O(1)	-0.36712(26)	0.34689(45)	0.26717(22)	29.7(20)	156.7(61)	32.2(14)	-4.7(28)	4.6(14)	-20.5(23)
O(2)	0.77095(28)	0.13998(44)	0.41400(23)	38.0(23)	131.0(54)	37.1(15)	13.8(28)	12.0(15)	-5.5(24)
O(3)	0.24428(23)	0.33124(33)	0.53327(17)	37.4(19)	74.1(38)	19.34(96)	-1.2(21)	4.4(11)	-7.9(15)
O(4)	0.10609(25)	0.23548(36)	0.47847(18)	39.0(20)	91.4(41)	19.4(10)	-7.8(23)	7.1(12)	-1.3(17)
O(5)	0.25926(28)	0.13449(35)	0.49762(18)	63.9(26)	68.0(37)	17.9(10)	10.3(25)	5.6(13)	1.0(16)
N(1)	0.00422(33)	0.34612(46)	0.33985(23)	35.1(26)	104.6(58)	23.2(14)	6.0(30)	4.5(15)	8.5(22)
N(2)	0.41778(31)	0.26575(45)	0.40007(24)	35.5(25)	82.4(51)	26.0(15)	0.5(27)	8.4(15)	2.1(21)
N(3)	0.34446(48)	0.38142(79)	0.24467(31)	70.5(43)	260.(12)	29.9(20)	-29.1(59)	22.9(24)	2.5(40)
N(4)	0.84765(43)	0.07665(54)	0.27473(30)	63.7(38)	116.4(67)	33.3(20)	-20.1(41)	4.9(22)	-15.1(29)
C(1)	0.08081(39)	0.33749(51)	0.35419(27)	37.2(31)	78.7(57)	18.7(15)	-2.0(33)	4.4(17)	7.2(23)
C(2)	0.34269(39)	0.28721(50)	0.39295(25)	42.7(31)	70.1(52)	17.3(13)	-5.1(32)	4.6(16)	0.5(21)
C(3)	0.28257(51)	0.34557(73)	0.25822(31)	56.1(41)	158.7(98)	18.8(16)	-10.6(51)	7.5(21)	-1.8(32)
C(4)	0.11418(48)	0.12771(65)	0.28681(31)	56.7(40)	97.9(70)	23.2(18)	-0.8(44)	6.9(22)	-5.7(29)
C(5)	0.20322(44)	0.30477(68)	0.27617(29)	46.2(35)	124.4(80)	19.3(15)	-14.5(44)	5.4(19)	-0.5(30)
C(6)	0.19955(40)	0.18890(63)	0.30141(28)	45.8(31)	104.2(68)	22.7(15)	-4.1(40)	7.4(18)	-20.6(28)
ME(1)	-0.41819(44)	0.43787(76)	0.28748(39)	34.0(34)	181.(11)	40.3(25)	12.6(48)	8.8(24)	-23.9(42)
ME(2)	0.84191(43)	0.20248(75)	0.45475(37)	34.6(33)	153.6(92)	38.8(24)	9.9(47)	7.4(23)	15.4(40)
HC(5)	0.1484(52)	0.3243(67)	0.2593(37)	5.2(21)					
HC(6)	0.2422(52)	0.1296(70)	0.3028(35)	7.6(21)					

[A] ESTIMATED STANDARD DEVIATIONS IN THE LEAST SIGNIFICANT FIGURE(S) ARE GIVEN IN PARENTHESES IN THIS AND ALL SUBSEQUENT TABLES. [B] THE FORM OF THE ANISOTROPIC THERMAL ELLIPSOID IS: EXP[-(B11H^2+B22K^2+B33L^2+2B12HK+2B13HL+2B23KL)]. THE QUANTITIES GIVEN IN THE TABLE ARE THE THERMAL COEFFICIENTS X 10^4.

Table III. Derived Parameters for the Rigid-Group Atoms of RhI(*trans*-H(NC)C=C(CN)H)P(OC$_6$H$_5$)$_3$(*p*-CH$_3$OC$_6$H$_4$NC)$_2$

ATOM	X	Y	Z	B,A^2	ATOM	X	Y	Z	B,A^2
R1C(1)	-0.08922(18)	0.34868(35)	0.32203(19)	3.77(12)	R3C(4)	0.51253(21)	0.35411(41)	0.63242(20)	5.29(15)
R1C(2)	-0.13656(25)	0.44199(30)	0.33932(19)	4.46(13)	R3C(5)	0.45469(29)	0.27476(38)	0.65088(18)	6.04(17)
R1C(3)	-0.23041(25)	0.44344(30)	0.32186(20)	4.58(13)	R3C(6)	0.36553(26)	0.26560(34)	0.61694(20)	5.00(14)
R1C(4)	-0.27692(18)	0.35158(36)	0.28712(20)	3.99(12)	R4C(1)	0.08045(28)	0.21244(40)	0.53367(17)	3.65(11)
R1C(5)	-0.22959(25)	0.25826(31)	0.26984(19)	4.79(14)	R4C(2)	0.03079(31)	0.29642(31)	0.55677(21)	5.48(15)
R1C(6)	-0.13574(25)	0.25681(30)	0.28729(20)	4.41(13)	R4C(3)	-0.00191(31)	0.27263(39)	0.60959(22)	6.27(18)
R2C(1)	0.50627(18)	0.23237(36)	0.40548(19)	3.58(11)	R4C(4)	0.01504(33)	0.16484(46)	0.63932(19)	5.77(16)
R2C(2)	0.57381(25)	0.27875(33)	0.45336(17)	4.05(12)	R4C(5)	0.06470(35)	0.08086(34)	0.61621(23)	6.89(19)
R2C(3)	0.66354(21)	0.24859(36)	0.45793(16)	4.21(13)	R4C(6)	0.09740(31)	0.10466(35)	0.56339(22)	6.12(17)
R2C(4)	0.68572(20)	0.17205(37)	0.41462(19)	4.02(12)	R5C(1)	0.27829(25)	0.04905(31)	0.45920(17)	3.51(11)
R2C(5)	0.61818(28)	0.12567(36)	0.36675(18)	5.47(15)	R5C(2)	0.21011(19)	-0.01334(36)	0.41904(19)	4.15(12)
R2C(6)	0.52845(24)	0.15583(37)	0.36218(17)	5.05(15)	R5C(3)	0.23189(25)	-0.10015(35)	0.38070(18)	5.26(15)
R3C(1)	0.33420(19)	0.33580(35)	0.56455(18)	3.26(11)	R5C(4)	0.32185(29)	-0.12457(34)	0.38252(19)	5.19(15)
R3C(2)	0.39205(26)	0.41515(33)	0.54610(16)	3.97(12)	R5C(5)	0.39002(20)	-0.06218(39)	0.42269(21)	5.15(15)
R3C(3)	0.48121(24)	0.42430(35)	0.58003(21)	5.01(14)	R5C(6)	0.36825(21)	0.02463(36)	0.46103(18)	4.26(13)

RIGID GROUP PARAMETERS

GROUP	X$_C$^{A}	Y$_C$	Z$_C$	DELTA^B	EPSILON	ETA
R1	-0.18307(18)	0.35013(24)	0.30458(12)	0.0057(24)	-2.6470(27)	0.0372(27)
R2	0.59600(18)	0.20221(23)	0.41005(12)	-0.4455(33)	-2.2749(27)	2.8926(35)
R3	0.42337(19)	0.34495(25)	0.59849(13)	-0.2256(32)	2.3880(27)	-2.7107(34)
R4	0.04774(19)	0.18864(29)	0.58649(15)	0.4225(30)	-3.1325(27)	-1.1615(27)
R5	0.30007(19)	-0.03776(24)	0.42086(12)	1.7543(24)	2.9947(24)	0.7309(27)

^{A} X$_C$, Y$_C$, AND Z$_C$ ARE THE FRACTIONAL COORDINATES OF THE ORIGIN OF THE RIGID GROUP. ^{B} THE RIGID GROUP ORIENTATION ANGLES DELTA, EPSILON, AND ETA (RADIANS) HAVE BEEN DEFINED PREVIOUSLY: S.J. LA PLACA AND J.A. IBERS, ACTA CRYSTALLOGR., 18, 511(1965).

Table IV. Root-Mean-Square Amplitudes of Vibration along Principal Ellipsoid Axes (Å)

Atom	Min	Intermed	Max
Rh	0.1810 (6)	0.1992 (6)	0.2116 (7)
I	0.2050 (6)	0.2404 (6)	0.2885 (6)
P	0.195 (2)	0.204 (2)	0.210 (2)
O(1)	0.181 (6)	0.249 (6)	0.345 (6)
O(2)	0.191 (6)	0.284 (6)	0.309 (6)
O(3)	0.190 (6)	0.207 (5)	0.240 (6)
O(4)	0.202 (6)	0.211 (6)	0.251 (6)
O(5)	0.201 (6)	0.209 (6)	0.275 (5)
N(1)	0.193 (7)	0.228 (7)	0.273 (7)
N(2)	0.196 (7)	0.232 (7)	0.247 (7)
N(3)	0.210 (9)	0.295 (9)	0.423 (10)
N(4)	0.219 (9)	0.293 (8)	0.310 (8)
C(1)	0.194 (8)	0.204 (8)	0.243 (9)
C(2)	0.198 (8)	0.208 (8)	0.230 (9)
C(3)	0.208 (9)	0.247 (9)	0.328 (10)
C(4)	0.224 (9)	0.253 (9)	0.263 (9)
C(5)	0.209 (8)	0.221 (9)	0.295 (9)
C(6)	0.184 (9)	0.226 (8)	0.296 (9)
Me(1)	0.186 (10)	0.272 (10)	0.378 (11)
Me(2)	0.193 (9)	0.280 (10)	0.340 (10)

rather than steric in nature. The angles at the O atoms average 124.1 (9)°, in good agreement with the results of other workers.[21-23] The exo angles of the phenyl rings at the O atoms are very close to 120° (Table V).

As noted above, the two isocyanide ligands occupy trans axial positions in the coordination sphere. The Rh–C(1) distance, 1.957 (6) Å, is not significantly different from the Rh–C(2) distance, 1.970 (6) Å. The average, 1.964 (6) Å, is intermediate between a range of 1.819 (5)–1.924 (14) Å found in a series of nickel–*tert*-butyl isocyanide complexes[26-29] and the range 2.05 (1)–2.151 (8) Å in two molybdenum–methyl isocyanide complexes.[30,31] The C(1)–Rh–C(2) angle as well as the angles at the nitrile C and N atoms are, as expected, very close to 180° (Table V). The averaged C≡N distance, 1.143 (7) Å, agrees well with comparable distances in *tert*-butyl isocyanide complexes.[26-29] The averaged N–C(phenyl) distance, 1.384 (6) Å, is ca. 0.07 Å shorter than the N–C(CH$_3$)$_3$ distances in *tert*-butyl isocyanide complexes[26-29] no doubt reflecting, in part, the difference in hybridization (sp^2 vs. sp^3) at the C atoms attached to the isocyanide N atoms. There is considerably more distortion in the exo angles of the phenyl rings at the methoxy terminus than at the isocyanide terminus (Table V). This is probably caused by van der Waals repulsion between the methyl and phenyl protons since the methoxy groups are coplanar with the phenyl rings. Why this repulsion is not relieved by a rotation about the O–C(phenyl) bond is not readily apparent from packing considerations. However, the short (phenyl)C–O distances[32] (average 1.349 (6) Å) would seem to suggest some involvement, perhaps π interaction, of the O atom with the aromatic ring. Such an interaction would account for the planarity of the anisole grouping. The angles at the methoxy O atoms (average 117.0 (5)°) may be rationalized either as a tendency toward sp^2 hybridization at O or as a result of repulsion between the methyl and phenyl protons. The average O–CH$_3$ distance, 1.43 (1) Å, is in good agreement with that expected[32] for an O–C(sp^3) bond.

The fumaronitrile (*trans*-1,2-dicyanoethylene = FN) ligand is symmetrically π bonded to the Rh atom through the olefinic, C(5)–C(6), bond. Both C(5) and C(6) are situated almost exactly in the equatorial plane of the trigonal-bipyramidal coordination sphere. The dihedral angle between the plane defined by Rh, I, and P and the one defined by Rh, C(5), and C(6) is 4.2 (4)° resulting in the displacement of C(5) and C(6) by 0.09 and 0.02 Å, respectively, from the Rh–I–P plane. Small displacements of this general order of magnitude are a common feature of trigonal-bipyramidal complexes of monoolefins and may be attributed to nonspecific packing effects.

The two Rh–C(olefin) distances (Table V) are not significantly different and average 2.139 (6) Å. This value is in satisfactory agreement with the average M–C(olefin) distance in the only other trigonal-bipyramidal complex involving FN reported to date, 2.110 (9) Å in IrH(CO)(FN)(P(C$_6$H$_5$)$_3$)$_2$.[33] These values may be compared with M–C(olefin) distances of 2.025 (6) and 2.162 (6) Å for the unsymmetrically π-bonded FN in Pt(FN)(P(C$_6$H$_5$)$_3$)$_2$.[34] Other cyanoolefin complexes from which useful comparisons of the M–C(olefin) bond length may be drawn are as follows: Pt(TCNE)(P(C$_6$H$_5$)$_3$)$_2$,[35] 2.11 (3) Å (average) (TCNE = (tetracyanoethylene); Ni(TCNE)(*t*-(CH$_3$)$_3$CN≡C)$_2$,[27] 1.954 (4) Å (average); IrBr(CO)(TCNE)(P(C$_6$H$_5$)$_3$)$_2$,[33a] 2.166 (15) Å (average); Fe(CO)$_4$(AC),[36] 2.10 (1) Å (average) (AC = acrylonitrile, cyanoethylene); Ni(AC)(P(*o*-CH$_3$C$_6$H$_4$O)$_3$)$_2$,[37]

Table V. Interatomic Distances (Å) and Angles (deg) in RhI(*trans*-H(NC)C=C(CN)H)($P(OC_6H_5)_3$)(*p*-$CH_3OC_6H_5NC)_2$[a]

Bonding Distances					
Rh-I	2.739 (2)		N(1)-R1C(1)	1.387 (6)	1.384
Rh-P	2.265 (2)		N(2)-R2C(1)	1.381 (6)	
Rh-C(1)	1.957 (6)	1.964[b]	R1C(4)-O(1)	1.343 (5)	1.349
Rh-C(2)	1.970 (6)		R2C(4)-O(2)	1.354 (6)	
Rh-C(5)	2.141 (6)	2.139	O(1)-Me(1)	1.433 (10)	1.429
Rh-C(6)	2.137 (6)		O(2)-Me(2)	1.424 (8)	
Rh-Ct[c]	2.013 (7)		C(5)-C(6)	1.444 (10)	
P-O(3)	1.597 (4)	1.599	C(5)-C(3)	1.436 (10)	1.442
P-O(4)	1.594 (4)		C(6)-C(4)	1.447 (9)	
P-O(5)	1.606 (4)		C(5)-HC(5)	0.86 (8)	0.90
O(3)-R3C(1)	1.383 (4)	1.377	C(6)-HC(6)	0.94 (8)	
O(4)-R4C(1)	1.382 (6)		C(3)-N(3)	1.131 (9)	1.139
O(5)-R5C(1)	1.367 (6)		C(4)-N(4)	1.147 (8)	
C(1)-N(1)	1.140 (7)	1.143			
C(2)-N(2)	1.146 (7)				
Nonbonding Distances					
I-P	3.910 (2)		C(1)-C(5)	2.839 (9)	
I-C(1)	3.349 (6)		C(2)-C(5)	2.926 (8)	
I-C(2)	3.436 (6)		C(1)-C(6)	2.916 (9)	
I-C(5)	3.737 (7)		C(2)-C(6)	2.829 (8)	
P-C(6)	3.794 (7)		Rh-HC(5)	2.49 (8)	
P-C(1)	3.002 (6)		Rh-HC(6)	2.75 (8)	
P-C(2)	3.023 (7)				
Bond Angles					
I-Rh-P	102.37 (5)		R1C(4)-O(1)-Me(1)	117.4 (5)	117.0
I-Rh-C(1)	89.4 (2)		R2C(4)-O(2)-Me(2)	116.6 (5)	
I-Rh-C(2)	92.3 (2)		Rh-P-O(3)	122.2 (2)	117.1
I-Rh-C(5)	99.2 (2)		Rh-P-O(4)	111.3 (2)	
I-Rh-C(6)	138.6 (2)		Rh-P-O(5)	117.9 (2)	
P-Rh-C(1)	90.3 (2)		O(3)-P-O(4)	99.1 (2)	100.9
P-Rh-C(2)	90.8 (2)		O(3)-P-O(5)	94.8 (2)	
P-Rh-C(5)	158.3 (2)		O(4)-P-O(5)	105.8 (2)	
P-Rh-C(6)	119.0 (2)		P-O(3)-R3C(1)	123.4 (3)	124.1
C(1)-Rh-C(5)	87.6 (2)		P-O(4)-R4C(1)	125.3 (3)	
C(1)-Rh-C(6)	90.8 (2)		P-O(5)-R5C(1)	123.5 (3)	
C(2)-Rh-C(5)	90.6 (2)		O(3)-R3C(1)-R3C(2)	120.2 (3)	119.9
C(2)-Rh-C(6)	87.0 (2)		O(3)-R3C(1)-R3C(6)	119.7 (4)	
C(1)-Rh-C(2)	177.7 (2)		O(4)-R4C(1)-R4C(2)	118.5 (4)	
C(5)-Rh-C(6)	39.5 (3)		O(4)-R4C(1)-R4C(6)	121.3 (4)	
I-Rh-Ct	118.9 (2)		O(5)-R5C(1)-R5C(2)	121.5 (4)	
P-Rh-Ct	138.7 (2)		O(5)-R5C(1)-R5C(6)	118.5 (3)	
C(1)-Rh-Ct	89.1 (2)		Rh-C(5)-C(6)	70.1 (3)	70.3
C(2)-Rh-Ct	88.7 (2)		Rh-C(6)-C(5)	70.5 (4)	
Rh-C(1)-N(1)	176.3 (6)	175.8	Rh-C(5)-C(3)	114.0 (4)	114.0
Rh-C(2)-N(2)	175.2 (5)		Rh-C(6)-C(4)	114.0 (4)	
C(1)-N(1)-R1C(1)	176.2 (6)	175.8	Rh-C(5)-HC(5)	104 (5)	
C(2)-N(2)-R2C(1)	175.4 (6)		Rh-C(6)-HC(6)	122 (5)	
N(1)-R1C(1)-R1C(2)	120.3 (4)	120.0	C(3)-C(5)-C(6)	121.0 (7)	
N(1)-R1C(1)-R1C(6)	119.7 (4)		C(4)-C(6)-C(5)	118.3 (6)	
N(2)-R2C(1)-R2C(2)	119.6 (4)		C(3)-C(5)-HC(5)	126 (5)	
N(2)-R2C(1)-R2C(6)	120.4 (3)		C(4)-C(6)-HC(6)	104 (5)	
R1C(3)-R1C(4)-O(1)	124.0 (4)	124.3	C(6)-C(5)-HC(5)	106 (5)	
R2C(3)-R2C(4)-O(2)	124.5 (3)		C(5)-C(6)-HC(6)	126 (5)	
R1C(5)-R1C(4)-O(1)	116.0 (4)	115.7	C(5)-C(3)-N(3)	177.7 (10)	177.9
R2C(5)-R2C(4)-O(2)	115.5 (4)		C(6)-C(4)-N(4)	178.1 (8)	
Conformational Angles					
C(4)-C(6)-C(5)-C(3)	146.0 (6) (γ)		HC(6)-C(6)-C(5)-Rh	116 (5)	
Rh-C(5)-C(6)-C(4)	107.4 (6) (δ)		HC(5)-C(5)-C(6)-Rh	99 (6)	
Rh-C(6)-C(5)-C(3)	106.6 (6) (δ)				
Vector-Plane Normal Angles					
[C(5)-C(6)]-[HC(6)-C(6)-C(4)]	60 (4) (β)		[C(6)-C(5)]-[HC(5)-C(5)-C(3)]	63 (5) (β)	

[a] The numbering system is as follows. The moiety N(1)-ring 1-O(1)-Me(1) is attached to C(1); similarly N(2)-ring 2-O(2)-Me(2) is attached to C(2). The moieties O(*n*)-ring *n*, *n* = 3-5, are attached to P. [b] These are average values. [c] Ct is defined as the midpoint of the olefinic (C(5)-C(6)) bond. Estimated uncertainties in the positional coordinates of Ct are taken to be those of C(5); see Table II.

2.016 (10) and 1.911 (12) Å. The Rh-Ct distance[38] in the present complex is 2.013 (7) Å.

The olefinic C(5)-C(6) bond length, 1.444 (10) Å, is ca. 0.10 Å longer than the expected value for the free olefin[33b] as a result of the synergistic σ-π interaction[39,40] with the metal center. The C(5)-C(6) distance is the same (within experimental error) as the olefinic C-C distance in IrH(CO)(FN)($P(C_6H_5)_3)_2$[33] and marginally shorter than the corresponding distance in Pt(FN)($P(C_6H_5)_3)_2$[34] and a series of TCNE complexes.[1,27,33a]

There is considerable angular distortion in the equatorial plane. The appropriate angular data are represented schematically in Figure 3. The most significant distortions are found in the P-Rh-Ct[41] and P-Rh-I angles which deviate by ca. 18°, respectively, above and below the expected 120°. The I-Rh-Ct angle, on the other hand, is very close to the expected value. This result suggests that the angular position of the $P(OC_6H_5)_3$ ligand in the equatorial plane is dictated primarily by steric considerations. Model building demonstrates convincingly that within the constraints imposed by the particular rotational conformer adopted by the $P(OC_6H_5)_3$ group in the solid state, a P–Rh–Ct angle of 120° would lead to impossibly close contacts between R5 of the $P(OC_6H_5)_3$ ligand and the terminal C≡N grouping (C(4), N(4)) of FN; see Figure 2. Modeling also reveals that a reorientation of the coordination sphere leading to an axial $P(OC_6H_5)_3$ in trigonal-bipyramidal geometry is sterically possible although certainly not as favorable as the equatorial configuration. This result is consistent with modeling experiments on $IrH(CO)(FN)(P(C_6H_5)_3$ for which it has been shown[33a] that an axial disposition for the two $P(C_6H_5)_3$ ligands is exceedingly unfavorable owing to steric repulsion between the phenyl rings of $P(C_6H_5)_3$ and FN. Such findings are also consistent with the cone-angle calculations of Tolman[42] which suggest that $P(OC_6H_5)_3$ is considerably less sterically demanding than $P(C_6H_5)_3$. The presence of the sterically innocuous iodo ligand in the equatorial plane is obviously of some import in allowing for the above noted angular distortions: replacement of the iodo ligand with $P(OC_6H_5)_3$ leads to extensive dissociation of FN in solution.[3] A similar effect is found in the corresponding $P(C_6H_5)_3$ complexes.[2] The internal angles of the three-membered metallocycle (Table V) are within 1σ of those found in $IrH(CO)(FN)(P(C_6H_5)_3)_2$[33] and midrange for a large number of monoolefin complexes.[1,16,27,37,43]

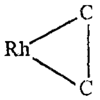

The angular distortions within the olefin itself are confined to a bending back (vide infra), away from the metal center, of the substituent H and C≡N. Aside from the lengthening of the central C═C bond of the olefin (vide supra), all other distances within the olefin are apparently unaffected by coordination. The average C–CN distance, 1.442 (10) Å, is in excellent agreement with 1.44 Å expected[32] for a sp^2(C)–(C)sp bond and 1.441 (5) Å in TCNE.[44,45] The two C≡N distances are equivalent and the average (Table V) is only marginally longer than the corresponding distance in TCNE.[45]

The deviations from planarity of the olefin may be conveniently described by the angles α and β given in Tables V and VI. Although no direct comparison of these angles with those in other FN complexes is possible, typical values for TCNE in five-coordinate Ir complexes are about 69° (α) and 56° (β).[46] Hence, as expected, the bending back of the olefin (as measured by 90° − β) is greater for the more highly activated olefin, TCNE.

Comparing $RhI(FN)(P(OC_6H_5)_3)(p\text{-}CH_3OC_6H_4NC)_2$ and $IrH(CO)(FN)(P(C_6H_5)_3)_2$[33b] we find little to distinguish the two metal–olefin interactions from a consideration of either the M–C distances, 2.139 (6) and 2.110 (9) Å, or the C═C distances, 1.444 (10) and 1.431 (20) Å. One therefore might conclude that the strength of the metal–olefin interaction is roughly the same in both complexes and rationalize this equivalence in terms of the disparity of the two donor sets fortuitously leading to equivalent electron-donating capability at the two metal centers. However, a comparison of the bending back of the coordinated FN groups in the two complexes indicates a difference in the strength of the metal–olefin interaction. Since the H atoms of the FN group in the Ir complex were not located, a comparison of the geometries of the two coordinated olefins must be made ignoring the H atom positions in the Rh complex. Convenient measures in this instance are the angles[46] δ and γ (Table V). The angle δ increases from 90° and the angle γ decreases from 180° as the bending back increases. These angles are 107 and 146° in the Rh complex and 112 and 136° in the Ir complex. Thus a stronger metal–olefin interaction appears likely in the Ir complex. This result is in line with the general expectation that Ir(I) is more electron rich than Rh(I) and hence capable of greater electron donation into the π* orbitals of the olefin. Such a result is consistent with the occurrence of rotation of the FN group in the present Rh(I) complex, since the barrier to olefin rotation should be a function of the magnitude of the π interaction.[47]

Table VI. Selected Weighted Least-Squares Planes in $RhI(trans\text{-}H(NC)C{=}C(CN)H)(P(OC_6H_5)_3)(p\text{-}CH_3OC_6H_4NC)_2$

$AX + BY + CZ = D^a$

Plane	A	B	C	D
1	14.75	−1.41	−0.27	2.58
2	−1.03	8.19	15.18	6.47
3	−2.62	−1.60	21.68	5.71

Distances (Å) of Various Atoms from Selected Planes

Atom	1	2	3
Rh	0.00 (0)		
I	0.00 (0)		
P	0.00 (0)		
C(3)		−0.01 (1)	
C(4)			0.00 (1)
C(5)	−0.08 (1)	0.01 (1)	
C(6)	0.02 (1)		0.00 (1)
N(3)		0.01 (1)	
N(4)			0.00 (1)
HC(5)		−0.03 (8)	
HC(6)			0.01 (7)

Dihedral Angle between Planes 2 and 3 = α = 54°

[a] Monoclinic coordinates.

Conclusions

The present structural results demonstrate convincingly that the solid-state configuration for the complex is trigonal bipyramidal with equatorial fumaronitrile rather than tetragonal pyramidal with apical fumaronitrile. The extension of this result to the solution configuration of $RhI(FN)(P(OC_6H_5)_3)(p\text{-}CH_3OC_6H_4NC)_2$ is fraught with uncertainty. It is, however, generally assumed that the solid-state geometry is equivalent to the solution ground-state geometry in the absence of specific solvation effects. If one is willing to accept this proposition, then the dynamic solution behavior of $RhI(FN)(P(OC_6H_5)_3)(p\text{-}CH_3OC_6H_4NC)_2$ and its $P(C_6H_5)_3$ analogue would be a rotation of the fumaronitrile accompanying an axial–equatorial interchange of the four remaining ligands of the trigonal-bipyramidal coordination sphere in the Berry pseudorotation mechanism.[48] Such an explanation would adequately account for the dynamic solution behavior of the complex.[2]

Acknowledgment. The authors wish to express their thanks to Dr. K. Kawakami and Professor T. Tanaka for providing the crystalline sample used in this study and for helpful discussions. This work was supported in part by the National Science Foundation.

Registry No. $RhI(trans\text{-}H(NC)C{=}C(CN)H)(P(OC_6H_5)_3)(p\text{-}CH_3OC_6H_4NC)_2$, 53992-82-8.

Supplementary Material Available. A listing of structure amplitudes and a table of idealized positions for the phenyl hydrogen atoms of $RhI(trans\text{-}H(NC)C{=}C(CN)H)(P(OC_6H_5)_3)(p\text{-}CH_3OC_6H_4NC)_2$ will appear following these pages in the microfilm edition of this volume of the journal. Photocopies of the supplementary material from this paper only or microfiche (105 × 148 mm, 24× reduction, negatives) containing all of the supplementary material for the papers in this issue may be obtained from the Business Office, Books and Journals Division, American Chemical Society, 1155 16th St., N.W., Washington, D.C. 20036. Remit check or money order for $4.50 for photocopy or $2.50 for microfiche, referring to code number AIC505139-12-75.

References and Notes

(1) J. S. Ricci and J. A. Ibers, *J. Am. Chem. Soc.*, **93**, 2391 (1971).
(2) T. Kaneshima, K. Kawakami, and T. Tanaka, *Inorg. Chem.*, **13**, 2198 (1974).
(3) K. Kawakami, K. Take-Uchi, and T. Tanaka, *Inorg. Chem.*, **14**, 877 (1975).
(4) P. W. R. Corfield, R. J. Doedens, and J. A. Ibers, *Inorg. Chem.*, **6**, 197 (1967).
(5) R. J. Doedens and J. A. Ibers, *Inorg. Chem.*, **6**, 204 (1967).
(6) J. A. Ibers, *Acta Crystallogr.*, **22**, 604 (1967).
(7) In addition to various local programs for the CDC 6400 computer, modified versions of the following programs were employed: Zalkin's FORDAP Fourier summation program, Johnson's ORTEP thermal ellipsoid plotting program, Busing and Levy's ORFFE error function program, Dewar's FAME normalized structure factor program, and the Main, Woolfson, and Germain direct-methods programs LSAM. Our full-matrix least-squares program NUCLS, in its nongroup form, closely resembles the Busing–Levy ORFLS program. Our absorption program, AGNOST, incorporates the Coppens–Leiserowitz–Rabinovich logic for Gaussian integration.
(8) D_{6h} symmetry, C–C = 1.392 Å, C–C–C = 120°.
(9) C–H = 0.95 Å, C–C–H = 120°.
(10) The source of f, $\Delta f'$, and $\Delta f''$ is "International Tables for X-Ray Crystallography", Vol. IV, Kynoch Press, Birmingham, England, 1974.
(11) Supplementary material.
(12) Throughout this paper the fumaronitrile ligand is considered to occupy one coordination site.
(13) M. R. Snow and J. A. Ibers, *Inorg. Chem.*, **12**, 224 (1973).
(14) D. J. Hodgson and J. A. Ibers, *Inorg. Chem.*, **8**, 1282 (1969).
(15) D. M. P. Mingos, W. T. Robinson, and J. A. Ibers, *Inorg. Chem.*, **10**, 1043 (1971).
(16) J. A. McGinnety, R. J. Doedens, and J. A. Ibers, *Inorg. Chem.*, **6**, 2243 (1967).
(17) P. B. Hitchcock, M. McPartlin, and R. Mason, *Chem. Commun.*, 1367 (1969).
(18) J. L. DeBoer, D. Rogers, A. C. Skapski, and P. G. H. Troughton, *Chem. Commun.*, 756 (1966).
(19) S. J. La Placa and J. A. Ibers, *Acta Crystallogr.*, **18**, 511 (1965).
(20) B. A. Frenz and J. A. Ibers, *MTP Int. Rev. Sci., Phys. Chem., Ser. One*, **11**, 33 (1972).
(21) H. L. Plastas, J. M. Stewart, and S. O. Grim, *Inorg. Chem.*, **12**, 265 (1973).
(22) H. S. Preston, J. M. Stewart, H. J. Plastas, and S. O. Grim, **11**, 161 (1972).
(23) F. A. Cotton, B. A. Frenz, and A. J. White, *Inorg. Chem.*, **13**, 1407 (1974).
(24) R. Mason and A. D. C. Towl, *J. Chem. Soc. A*, 1601 (1970).
(25) A. P. Gaughan, Jr., Z. Dori, and J. A. Ibers, *Inorg. Chem.*, **13**, 1657 (1974).
(26) R. S. Dickson and J. A. Ibers, *J. Organomet. Chem.*, **36**, 191 (1972).
(27) J. K. Stalick and J. A. Ibers, *J. Am. Chem. Soc.*, **92**, 5333 (1970).
(28) R. S. Dickson and J. A. Ibers, *J. Am. Chem. Soc.*, **94**, 2988 (1972).
(29) D. J. Yarrow, J. A. Ibers, Y. Tatsuno, and S. Otsuka, *J. Am. Chem. Soc.*, **95**, 8590 (1973).
(30) M. Novotny, D. F. Lewis, and S. J. Lippard, *J. Am. Chem. Soc.*, **94**, 6961 (1972).
(31) R. D. Adams, M. D. Brice, and F. A. Cotton, *J. Am. Chem. Soc.*, **95**, 6594 (1973).
(32) Assuming the following covalent radii: C(sp^3), 0.77 Å; C(sp^2), 0.74 Å; C(sp), 0.70 Å; O, 0.66 Å. See F. A. Cotton and G. Wilkinson, "Advanced Inorganic Chemistry", 3rd ed, Wiley, New York, N.Y., 1972.
(33) (a) Lj. Manojlovic-Muir, K. W. Muir, and J. A. Ibers, *Discuss. Faraday Soc.*, **47**, 84 (1969); (b) K. W. Muir and J. A. Ibers, *J. Organomet. Chem.*, **18**, 175 (1969).
(34) Values quoted in ref 33a
(35) C. Panattoni, G. Bombieri, U. Belluco, and W. H. Baddley, *J. Am. Chem. Soc.*, **90**, 798 (1968).
(36) A. R. Luxmoore and M. R. Truter, *Acta Crystallogr.*, **15**, 1117 (1962).
(37) L. J. Guggenberger, *Inorg. Chem.*, **12**, 499 (1973).
(38) Ct is defined as the midpoint of the olefinic bond, C(5)–C(6). The Rh–Ct distance is only meaningful for comparison purposes when the olefin is symmetrically bonded to the metal center.
(39) M. J. S. Dewar, *Bull. Soc. Chim. Fr.*, **C79**, 18 (1951).
(40) J. Chatt and L. A. Duncanson, *J. Chem. Soc.*, 2939 (1953).
(41) Ideally 120° in the equatorial plane of a perfect trigonal bipyramid if the olefin occupies one coordination site at Ct.
(42) C. A. Tolman, *J. Am. Chem. Soc.*, **92**, 2956 (1970).
(43) See Table III of ref 33a.
(44) An X-Ray structure determination of fumaronitrile has not yet been undertaken.
(45) Quoted in Table VI of ref 27.
(46) S. D. Ittel and J. A. Ibers, *Adv. Organomet. Chem.*, in press.
(47) K. S. Wheelock, J. H. Nelson, L. C. Cusachs, and H. B. Jonassen, *J. Am. Chem. Soc.*, **92**, 5110 (1970).
(48) E. L. Muetterties, *Acc. Chem. Res.*, **1**, 136 (1968).

Contribution from the Departments of Chemistry, Tulane University, New Orleans, Louisiana 70118, and The University of Alabama, University, Alabama 35486

Electron Paramagnetic Resonance Spectra of Vanadium(II) and Nickel(II) Doped into Crystals of Cesium Cadmium Chloride and a Redetermination of the Structure of Cesium Cadmium Chloride[1]

JIN RONG CHANG,[2a] GARY L. McPHERSON,*[2a] and JERRY L. ATWOOD*[2b]

Received June 26, 1975

AIC504483

The crystal structure of $CsCdCl_3$ has been redetermined using diffractometer-measured intensity data. The compound crystallizes in the hexagonal space group $P6_3/mmc$ with unit cell dimensions of $a = 7.403$ (2) Å and $c = 18.406$ (3) Å. Based on 354 observed reflections the structure was refined by full-matrix least-squares methods to R_1 and R_2 values of 0.044 and 0.050, respectively. There are two crystallographically distinct types of cadmium ions in $CsCdCl_3$. One of the cadmium ions, Cd(1), occupies a site having D_{3d} symmetry, while the other, Cd(2), exhibits C_{3v} site symmetry. The coordination sphere of Cd(1) contains six equivalent chloride ions which form a nearly perfect octahedron with a cadmium–chloride separation of 2.598 Å. In contrast, the coordination sphere of Cd(2) contains two distinct groups of chloride ions which form a noticeably distorted octahedron; the cadmium–chloride distances are 2.639 and 2.588 Å. The EPR spectrum of $CsCdCl_3$ doped with V(II) shows that both types of cadmium ion are replaced. The spectrum can be satisfactorily interpreted with an axial spin Hamiltonian. An analysis of the spin Hamiltonian parameters indicates that 90–95% of the V(II) ions enter sites normally occupied by Cd(1) while the remaining 5–10% enter the sites that would contain Cd(2). The spectrum of $CsCdCl_3$ containing Ni(II) shows resonances from only one kind of Ni(II) ion which suggests that only one of the two sites is occupied.

Introduction

When crystallized from the melt, $CsCdCl_3$ adopts a hexagonal lattice in which there are two crystallographically distinct types of cadmium ions.[3] Both cadmium ions (1 and 2) are surrounded by octahedra of chloride ions. Two octahedra containing type 2 cadmium ions share a face forming a $Cd_2Cl_9^{5-}$ unit which then shares corners with six different octahedra containing type 1 cadmium ions. Figure 1 shows a simplified view of the $CsCdCl_3$ structure. The point symmetry at cadmium 1 is D_{3d} while it is C_{3v} at cadmium 2. This structure can be considered as intermediate between the $CsNiCl_3$ structure which consists of infinite linear arrays of octahedra sharing faces and the perovskite structure which consists of a three-dimensional network of octahedra sharing corners.

An investigation of the EPR spectra of single crystals of